Research Article

Structural Basis for the Interaction Between Yeast Chromatin Assembly Factor 1 and Proliferating Cell Nuclear Antigen

Keely S. Orndorff [1], Evan J. Veltri [1], Nicole M. Hoitsma [2,4,5], Ivy L. Williams [1], Ian Hall [1], Grace E. Jaworski [1], Grace E. Majeres [1], Samaya Kallepalli [1], Abigayle F. Vito [1], Lucas R. Struble [3], Gloria E. O. Borgstahl [3] and Lynne M. Dieckman [1,*]

*1 - **Department of Chemistry and Biochemistry,** Creighton University, Omaha, NE, USA*
*2 - **Department of Biochemistry and Molecular Biology,** Department of Cancer Biology, University of Kansas Medical Center, Kansas City, KS, USA*
*3 - **The Eppley Institute for Research in Cancer and Allied Diseases,** Fred & Pamela Buffett Cancer Center, University of Nebraska Medical Center, Omaha, NE, USA*
*4 - **Department of Biochemistry,** University of Colorado at Boulder, Boulder, Colorado*
*5 - **Howard Hughes Medical Institute,** Chevy Chase, Maryland*

***Correspondence to Lynne M. Dieckman:** lynnedieckman@creighton.edu (L.M. Dieckman)*
https://doi.org/10.1016/j.jmb.2024.168695
Edited by Sepideh Khorasanizadeh

Abstract

Proliferating cell nuclear antigen (PCNA), the homotrimeric eukaryotic sliding clamp protein, recruits and coordinates the activities of a multitude of proteins that function on DNA at the replication fork. Chromatin assembly factor 1 (CAF-1), one such protein, is a histone chaperone that deposits histone proteins onto DNA immediately following replication. The interaction between CAF-1 and PCNA is essential for proper nucleosome assembly at silenced genomic regions. Most proteins that bind PCNA contain a PCNA-interacting peptide (PIP) motif, a conserved motif containing only eight amino acids. Precisely how PCNA is able to discriminate between binding partners at the replication fork using only these small motifs remains unclear. Yeast CAF-1 contains a PIP motif on its largest subunit, Cac1. We solved the crystal structure of the PIP motif of CAF-1 bound to PCNA using a new strategy to produce stoichiometric quantities of one PIP motif bound to each monomer of PCNA. The PIP motif of CAF-1 binds to the hydrophobic pocket on the front face of PCNA in a similar manner to most known PIP-PCNA interactions. However, several amino acids immediately flanking either side of the PIP motif bind the IDCL or C-terminus of PCNA, as observed for only a couple other known PIP-PCNA interactions. Furthermore, mutational analysis suggests positively charged amino acids in these flanking regions are responsible for the low micromolar affinity of CAF-1 for PCNA, whereas the presence of a negative charge upstream of the PIP prevents a more robust interaction with PCNA. These results provide additional evidence that positive charges within PIP-flanking regions of PCNA-interacting proteins are crucial for specificity and affinity of their recruitment to PCNA at the replication fork.

Introduction

DNA maintenance pathways such as replication, repair, and recombination are coordinated both spatially and temporally in an extraordinarily accurate manner. These processes involve the function of an incredibly large number of proteins, which each act on the DNA substrate only when needed. Access to the replication fork by these many players is dynamic and regulated by the replication accessory protein, proliferating cell nuclear antigen (PCNA).[1–7] PCNA functions as a scaffold during DNA-templated processes, coordinating the activities of these diverse replication, repair, and recombination factors.

PCNA is a ring-shaped, homotrimeric protein that encircles DNA. Each identical subunit is composed of two similar domains that are connected by a long, flexible loop called the inter-domain connecting loop (IDCL).[8] Once loaded onto DNA, PCNA will recruit other protein factors via an interaction on its front face (i.e., the side of PCNA facing the direction of DNA replication).[1,9] Proteins that interact with PCNA typically do so using a small motif called the PCNA-interacting peptide motif, or PIP motif. The canonical PIP motif is eight amino acids in length, comprising the consensus sequence Qxxhxxaa, where an "x" represents any amino acid, "h" represents a hydrophobic amino acid, and "a" represents an aromatic residue (usually phenylalanine). The sequences of PIP motifs in several PCNA-binding proteins are shown in Figure 1A. Canonical PIP motifs bind in a hydrophobic pocket on the front face of PCNA. The glutamine in position 1 of the PIP motif inserts into a small "Q pocket" in domain 2 near the C-terminus of PCNA. In addition to the hydrophobic residue in position 4, the aromatic residues in positions 7 and 8 typically form a 3_{10} helix that binds to the large hydrophobic pocket on the front face of PCNA near the IDCL.

Prior to DNA replication, nucleosomes established ahead of the replication fork must be disassembled. Nucleosomes are reformed on the newly synthesized DNA immediately after replication in a process called replication-coupled nucleosome assembly. The newly formed nucleosomes must contain the same histone post-translational modifications as the parent strand to maintain proper chromatin structure and gene expression. A major player in replication-coupled nucleosome assembly is the histone chaperone chromatin assembly factor 1 (CAF-1), which deposits H3-H4 tetramers bearing specific covalent modifications that promote gene silencing.[10–14] CAF-1 recruitment to the replication fork and subsequent histone deposition requires its association with PCNA.[15–18] This interaction is mediated by a PIP motif on CAF-1.

CAF-1 is a heterotrimeric protein. In yeast, it is composed of the subunits Cac1, Cac2, and Cac3, each named based on molecular weight. The PIP motif of CAF-1 exists within the largest subunit, Cac1.[17] As with the other two subunits of CAF-1, the structure of Cac1 has not been determined, but it contains several other regions important for CAF-1 function (Figure 1B). This includes two DNA-interacting regions (a basic domain called the KER domain that consists of many lysine, glutamic acid, and arginine residues[19–21] and a winged-helix domain (WHD) near the C-terminus),[19–20] two regions that interact with the smaller subunits of CAF-1 (a Cac2-binding region and a Cac3-binding region),[19,22–24] and a region believed to interact with histones (an acidic region referred to as the ED domain).[19,23] Although PIP motifs are often located near the C-terminus of PCNA-binding proteins, the PIP motif of Cac1 resides closer to the center of the subunit, between the KER and the Cac3-binding regions.

Disruption of the CAF-1-PCNA interaction inhibits CAF-1-mediated heterochromatin silencing and chromatin assembly during both DNA replication and repair.[13,17,24–27] However, precisely how PCNA chooses CAF-1 to access the replication fork during replication-coupled nucleosome assembly and the mechanism of binding between these two proteins are not well

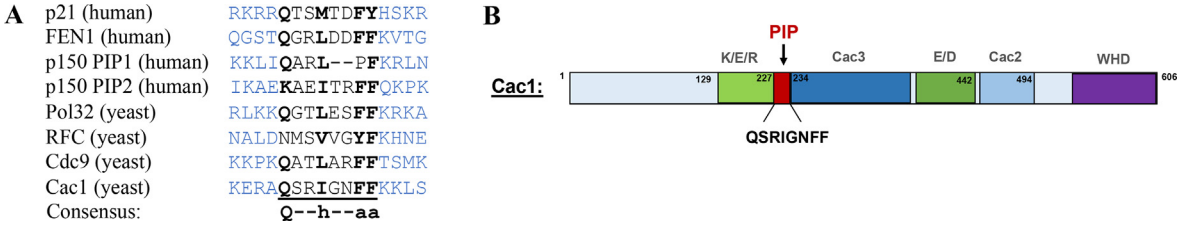

Figure 1. PIP motifs of various proteins. (A) Alignment of several PIP motifs of proteins in human and yeast. Residues within PIP sequences are indicated in black and residues flanking the PIP motif are indicated in blue. The PIP consensus sequence is displayed below the corresponding residues within the motif. Both PIP motifs within the human CAF-1 protein (p150) are shown. The PIP motif for RFC (replication factor C) is within the first and largest of five subunits (subunit 1) of RFC. (B) Linear representation of motifs and domains within the Cac1 subunit. The K/E/R region, Cac3-binding domain, E/D region, Cac2 binding domain, and winged-helix domain (WHD) are all shown. The PIP motif is shown in red.

understood. We characterized the interaction between yeast PCNA and CAF-1 using structural, kinetic, and thermodynamic studies. We used a novel strategy to produce pure complexes of the CAF-1 PIP motif bound to PCNA in a stoichiometric ratio of 1:1 (PIP:PCNA monomer). This was accomplished by fusing the sequence of the PIP motif of CAF-1 to the C-terminus of PCNA via a 5 amino acid linker, which allowed enough space and flexibility for each PIP motif to bind a PCNA monomer. We solved the crystal structure of this complex and determined the PIP motif of CAF-1 binds to the hydrophobic pocket on the front face of PCNA in the same way as most known PIP-PCNA interactions. Similar to a small number of other known PIP-PCNA interactions such as p21 and FEN1, the amino acids immediately flanking the PIP motif of CAF-1 interact with residues within the IDCL or C-terminus of PCNA; however, to a lesser extent than observed between PCNA and p21 or FEN1.[28,29] The affinity of the CAF-1 PIP-PCNA interaction was determined to be in the low micromolar range, as determined by both isothermal titration calorimetry (ITC) and surface plasmon resonance (SPR). Finally, mutational analysis suggests positively charged amino acids immediately C-terminal and N-terminal to the PIP motif of CAF-1 are responsible for the affinity to PCNA, whereas the presence of a negative charge upstream of the PIP prevents an even more robust interaction with PCNA. These results provide additional evidence that PIP-flanking residues, especially those with positively charged side chains, are required for specificity and affinity of the PCNA-PIP interaction.

Materials and Methods

Protein expression and purification.

Wild type yeast PCNA was N-terminally His_6-tagged, overexpressed in Bl21(DE3) bacteria harboring plasmid pKW336, and purified as described previously.[30] To produce the PCNA-PIP fusion protein, a five amino acid linker (GGSGG) and the sequence of the PIP motif of yeast CAF-1 (AKERAQSRIGNFFKKLSDS) were cloned, respectively, in frame, at the C-terminus of the gene encoding PCNA in the plasmid pKW336. The fusion protein was overexpressed in BL21(DE3) cells. Cells were lysed via sonication and the cell lysate was subjected to centrifugation for clarification. The PCNA-PIP fusion protein was purified using Ni-NTA agarose affinity chromatography (Thermo Scientific), DEAE anion exchange chromatography (GE Healthcare), and a Superdex 200 size exclusion chromatography column (GE Healthcare). All wildtype and mutant CAF-1 PIP peptides used in this work were commercially synthesized by GenScript. A tryptophan residue was added to the N-terminus of all peptides for quantification purposes.

Crystallization and structural determination.

The CAF-1 PIP-PCNA fusion protein was concentrated to a final concentration of 16.6 mg/ml for crystallization. Crystals were generated using the hanging-drop method at 18 °C with a reservoir solution of 0.1 M magnesium acetate tetrahydrate and 11% w/v PEG3350. For X-ray diffraction, crystals were transferred to a cryosolution containing reservoir solution with the addition of 25% ethylene glycol. The crystals were flash frozen and data was collected at 100 K on a Rigaku MicroMax-007 HF rotating anode diffractometer equipped with a Dectris Pilatus3R 200 K-A detector system at a wavelength of 1.54 Å. The X-ray data was collected using 60 s frames at a distance of 75 mm. Data were processed and scaled with the HKL3000R software package. Molecular replacement was conducted using the published structure of wildtype, uncomplexed PCNA (PDB 1PLQ). Structural refinement and model building were conducted in PHENIX1.19.2.[31] and Coot,[32] respectively. The final model and structure factors were deposited in the PBD (PDB entry: 8THW).

Isothermal titration calorimetry

Isothermal titration calorimetry (ITC) analyses were performed in a Nano ITC Low Volume calorimeter (TA Instruments) at a constant temperature of 310.15 K. The CAF-1 PIP peptide (WEAKERAQSRIGNFFKKLSDSNT) was placed into the sample cell at a concentration of 70 μM, and PCNA was used as the titrant at a concentration of 420 μM. A 6:1 ratio of titrant to sample cell was maintained for each trial. Both proteins were dialyzed in 100 mM HEPES, pH 7.4, 50 mM arginine, and 50 mM glutamic acid and degassed. The titrant was injected into the sample cell in a sequence of 24 injections of 2 μL each with 150 s of space between injections, with an initial injection of 1 μL that was discarded from calculations. The stir rate of the sample cell was set to 250 rpm. ITC data was fitted to obtain the binding isotherms with the software NanoAnalyze using an independent sites model. Blank experiments of PCNA into buffer were subtracted from the interaction experiments. To ensure reproducibility, five independent experiments from three different preparations of PCNA were carried out.

Surface plasmon resonance.

Surface plasmon resonance (SPR) assays were performed using a Biacore 8 K (Cytiva). Experiments were carried out at a flow rate of 30 μL/min at 25 °C in 10 mM HEPES, pH 7.4, 300 mM NaCl, 3 mM EDTA, 0.05% surfactant P20, and 1 mM DTT as the running buffer. His_6-tagged PCNA was immobilized on an NTA Series

S sensor chip. The chip surface was first activated using an injection of 350 mM EDTA (30 μL/min) followed by an injection of 0.5 mM $NiCl_2$ (10 μL/min). Increasing concentrations of the synthetic PIP peptide (WEAKERAQSRIGNFFKKLSDSNT) in running buffer were injected over the immobilized PCNA. Contact time for the PIP peptide was set to 60 s and dissociation time was 180 s. The signal from buffer alone (containing no peptide) over a reference flow cell was subtracted from all responses. Kinetic binding constants were determined using non-linear least-squares fitting to a two-state binding model with the Biacore Insight Evaluation 5.0 software. Steady state binding constants were obtained by fitting equilibrium data to a non-linear regression with the Biacore Insight Evaluation 5.0 software. Experiments were performed in triplicate using multiple PCNA protein preparations.

Enzyme-Linked immunosorbent assays

The wells of a 96 well EIA/RIA plate (Corning) were coated with 2 μg of PCNA in PBS (4.3 mM Na_2HPO_4, 1.4 mM KH_2PO_4, pH 7.4, 137 mM NaCl, 2.7 mM KCl) for 1 h. The wells were then washed four times with PBS, 0.05% Tween-20, blocked for 2 h with PBS with 5% milk, and washed again. Various amounts of the wildtype or mutant, biotinylated PIP peptides (see Table 2) (1–20 μg or 1–100 μg) in PBS with 5% milk were then added to the wells and incubated for 1 h. After washing, a 1:500 dilution of a biotin polyclonal antibody conjugated with horseradish peroxidase (Invitrogen) in PBS with 5% milk was added and incubated at 4 °C for 16–18 h. The plate was washed and 100 μL of ABTS Single Solution (Invitrogen) was added. Absorbance was measured at 415 nm after various amounts of time (5–30 min) using a BioTek Synergy H1 microplate reader (Agilent). Negative control reactions using bovine serum albumin instead of PCNA were carried out, and these background absorbance values were subtracted from the absorbance of each sample at the corresponding PIP peptide concentration. Positive controls using 1 μg and 2 μg of each PIP peptide was simultaneously carried out during every experiment to verify absorbance was similar for all wildtype and mutant peptides. Unless otherwise noted, all steps were performed at 25 °C.

Gene silencing assays using flow cytometry

A yeast strain containing a deletion of the endogenous *cac1* gene (W303, *cac1Δ::leu2, rtt106::kan, hmr::GFP/URA3*) and a pRS313-derived yeast expression plasmid for the wildtype Cac1 protein were kindly provided by Bruce Stillman. A Q5 Site-Directed Mutagenesis Kit (NEB) was used with the yeast expression plasmid as a template to generate plasmids with mutations in the *cac1* gene encoding for the following mutant Cac1 proteins: K223A, E224A, R225A, R229A, I230A, FF233/234AA, K235A, and K236A. The *cac1Δ* yeast cells were then transformed with either the wildtype plasmid or one of the mutant Cac1 plasmids using the Frozen-EZ Yeast Transformation kit (Zymo Research). For controls, yeast cells were left untransformed or transformed with the pRS313 empty vector. Cells were grown in 3 mL of liquid yeast peptone dextrose (YPD) media overnight with incubation at 30 °C and shaking at 200 rpm. Overnight cultures were used to inoculate fresh 10 mL cultures to $OD_{600} \approx 0.2$ and were grown with the same incubation conditions to $OD_{600} \approx 0.7$ (early log phase). Cells were pelleted by centrifugation at 4500 rpm for 5 min at 4 °C. The cell pellets were washed 3x with 2 mL of 1x PBS (137 mM NaCl, 2.7 mM KCl, 10 mM Na_2HPO_4, 1.8 mM KH_2PO_4 pH = 7.4) by resuspension and pelleting using the centrifugation conditions described above. Intercellular aggregates were diminished by water bath sonication (Bransonic CPX2800H) for 5 min at 25 °C on the low power setting. 20 – 50 μL of sonicated yeast cells were added to 1 mL 1x PBS and 1 μL of propidium iodide (PI) (invitrogen) and incubated at 25 °C in the dark for 15 min. The cells were pelleted by centrifugation at 1200 rpm for 5 min and excess PI in the supernatant was decanted. An additional 1 mL of fresh 1x PBS was used to resuspend the PI treated yeast. For each culture, 200 ul of cell suspension was acquired using a ZE5 flow cytometer (Biorad) enabled with a Forward Scatter Small Particle Detector (FSc spd). Data analysis of generated Flow Cytometry Standard (FCS) files was performed using Flowjo Version 10. For this, sequential gating was carried out to first exclude doublets. Next, dead cells were removed through exclusion of PI positive staining cells. Finally, estimations of the percent frequency of GFP expressing yeast were carried out. Experiments were run in duplicate using two independent yeast preparations.

Accession number

PDB: 8THW.

Results

Generation of the PCNA-CAF-1 PIP complex

To gain structural insight into the interaction between PCNA and CAF-1, we sought to obtain a pure complex of PCNA bound to the PIP motif of CAF-1 for use in X-ray crystallography. However, one PCNA trimer contains three potential binding sites for PIP motifs. Acquiring large amounts of pure protein complexes for structural determination, especially in proper stoichiometric ratios, is often difficult. To circumvent this, we

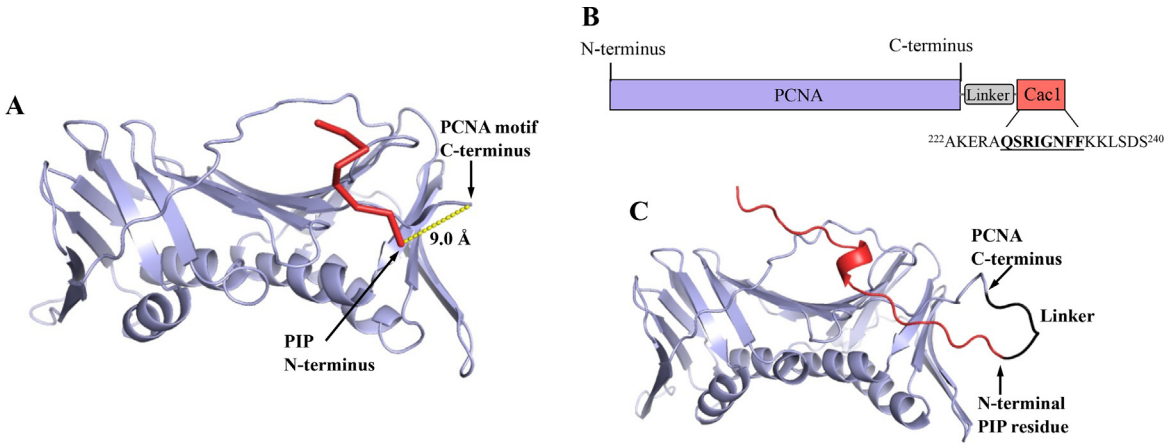

Figure 2. Rationale and generation of a novel fusion PCNA-PIP protein. (A) A PCNA monomer (light purple) bound to a representative PIP motif (red) (from yeast DNA ligase I; PDB 2OD8). The distance between the C-terminus of the PCNA monomer and the N-terminal residue of where a PIP motif would bind is shown with a yellow dotted line. (B) Linear representation of the fusion protein used to generate crystals. The sequence of the Cac1 PIP motif (bolded and underlined) and several flanking residues are represented as red, the five amino acid linker is shown in grey, and the PCNA monomer is shown in light purple. (C) AlphaFold2 predicted structure of the fusion protein sequence from (B). The PIP motif and flanking residues of Cac1 (red) is bound in the canonical PIP-binding pocket on PCNA (light purple) while fused to the C-terminus of PCNA via a linker (grey).

created a fusion protein construct containing one CAF-1 PIP motif per PCNA monomer. As shown in Figure 2A, the C-terminus of PCNA is in very close proximity to the PIP-binding region. In fact, in the crystal structure of PCNA, the C-terminus is only 9 Å from the hydrophobic pocket where the first residue in the consensus PIP motif (glutamine) binds. Therefore, we created a peptide where the PIP sequence of CAF-1 was fused in frame, via a five amino acid linker, to the C-terminus of the PCNA monomer (Figure 2B). Five or six amino acids N-terminally or C-terminally flanking the PIP motif, respectively, were also included in the sequence. Based on the length of the average amino acid, the linker should provide sufficient length and flexibility for the PIP motif to interact with the PIP-binding pocket on PCNA. This was verified by AlphaFold2.[33,34] The sequence of the PCNA-linker-CAF-1 PIP fusion construct was input into the AlphaFold2 software, and the predicted structure is shown in Figure 2C.

Structure of the interaction between PCNA and CAF-1

Using X-ray crystallography, we solved the structure of the complex formed between PCNA and the PIP motif of CAF-1 to a resolution of 2.6 Å (Table 1). The asymmetric unit contains three PIP motifs bound to one PCNA trimer (Figure 3A), with electron density for thirteen residues of Cac1, including density for all side chains of the eight PIP residues (Figure 3B). The structure of PCNA is largely unaltered upon binding to the PIP motif of CAF-1, with exceptions only in regions within and near the PIP-binding pocket (the overall RMSD is 0.846 Å for PCNA alone, PDB 1PLQ, compared to the PIP-bound structure). The PIP interacts with PCNA at the canonical PIP-binding pocket, and all PIP residues (QSRIGNFF) are in

Table 1 Data collection and refinement statistics.

Data Collection	
Space group	C121
Unit-cell parameters	
a (Å)	151.62
b (Å)	87.36
c (Å)	76.51
α (°)	90.00
β (°)	108.33
γ (°)	90.00
Resolution (Å)	25.00–2.6
R_{meas} (%)	0.063
$I/\sigma(I)$	17.2
cc1/2	(0.634)
Completeness (%)	99.2 (96.8)
Redundancy	4.5 (2.0)
Refinement	
Resolution (Å)	24.89–2.60
No. reflections	35,217
R_{work}/R_{free}	21.6/26.7
No. atoms	
Protein	6315
B-factors (Å^2)	
Protein	43.91
R.m.s deviations	
Bond length (Å)	0.009
Bond angles (°)	1.355
PDB ID	8THW

Values in parentheses are for highest-resolution shell.

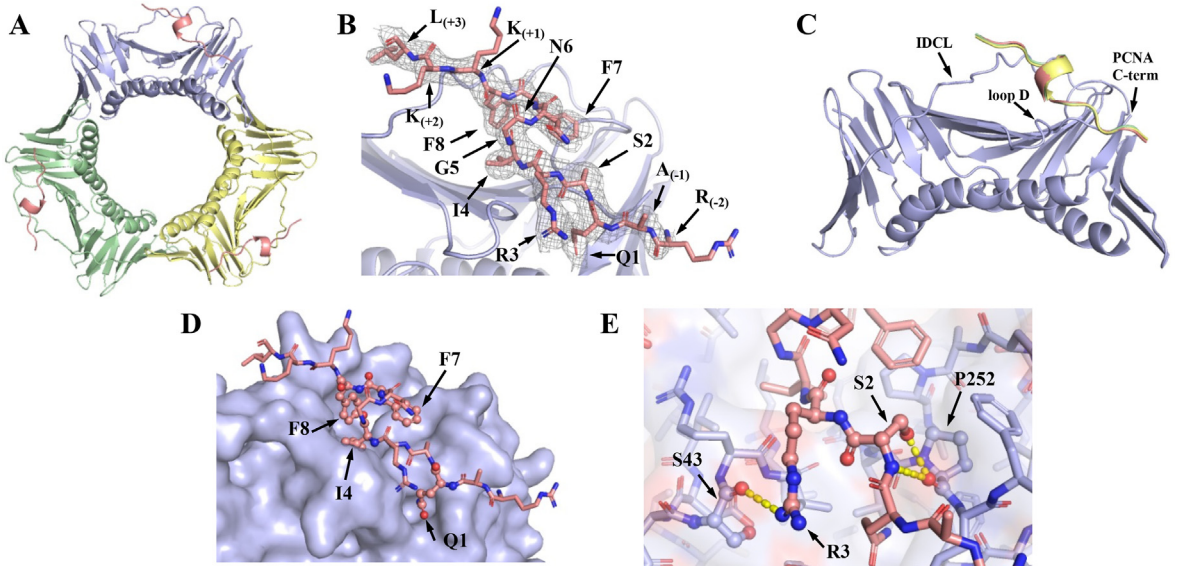

Figure 3. Crystal structure of the CAF-1 PIP motif bound to PCNA. (A) Three PIP motifs (pink) bound to one PCNA trimer are present in the asymmetric unit. Each subunit of PCNA is represented by a different color (purple, green, yellow). (B) Electron density for residues of the PIP motif of CAF-1. The Fo-Fc omit electron density map was contoured at 2.0 σ (shown as grey mesh), surrounding the PIP and flanking residues of CAF-1 (shown as pink sticks). All residues with observed density are labeled, including numbers showing positions relative to the PIP motif (a subscript negative number indicates an amino acid upstream of the PIP motif, a superscript positive number indicates an amino acid downstream of the PIP motif). (C) Alignment of the three PCNA monomers and three bound PIP motifs (pink, green, and yellow) from the trimeric structure. The IDCL, loop D, and C-terminus of PCNA are indicated. (D) Close up of the PIP motif bound to the hydrophobic pocket on the front face of PCNA. The conserved PIP residues are shown as spheres bound to the surface-view of PCNA. (E) Close up of the non-conserved PIP residues and interactions with PCNA. Polar contacts observed in every PIP-PCNA monomer are indicated as yellow dotted lines.

identical positions in all three bound motifs (Figure 3C). The glutamine in position 1 (Q1) of the PIP motif is inserted into the small "Q pocket" in domain 2 near the C-terminus of PCNA, and the other conserved residues – including the hydrophobic isoleucine in position 4 (h4) and phenylalanines in positions 7 and 8 (F7 and F8) – form the typical 3_{10} helix that bind to the large hydrophobic pocket between domains 1 and 2 of PCNA near the IDCL (Figure 3D).

In addition to the interactions typically seen with the four conserved amino acids in PIP motifs, other polar contacts are observed among the non-conserved amino acids in the PIP motif of CAF-1 (Figure 3E). The serine in position 2 (S2) of the PIP motif hydrogen bonds to the backbone of P252 in PCNA (located near the C-terminus of PCNA). The arginine sidechain in position 3 (R3) of the PIP motif also forms a hydrogen bond with the backbone of S43 in PCNA (located in loop D, on the front face of PCNA between domains 1 and 2 and below the PIP-binding site). These interactions between PCNA and S2 or R3 are observed in all three monomers within the crystal structure. The glycine and asparagine in positions 5 and 6 of the PIP motif, respectively, do not appear to make any polar contacts with PCNA.

Unexpectedly, electron density was observed for several CAF-1 amino acids flanking either side of the PIP motif, including two upstream (^{225}RA^{226}) and three downstream (^{235}KKL^{237}). Density for these five residues was observed in each of the three PIP motifs bound to the PCNA trimer. The position of the peptide backbone for these five additional residues showed minimal variability between the three bound PIP motifs (Figure 3C). However, the B-factors for these residues varied among the three motifs more so than those of the residues within the PIP motif (Figure 4A). Despite this, a number of polar contacts are observed between the PIP-flanking residues and PCNA. The backbones of both the R225 and the A226 residues upstream of the PIP motif hydrogen bond with residues in PCNA, although the specific amino acids contacted in PCNA by these residues vary slightly among monomers. In all three monomers, however, contacts exist between the backbone of either R225 and/or A226 and F254 in PCNA (Figure 4B). F254 is the most C-terminal amino acid visible in PCNA in our structure. Notably, the position of the α-carbon of F254 is shifted by ~3.0 Å compared to its position in the structure of PCNA alone (PDB 1PLQ). Density for the four C-terminal amino acids in PCNA are not

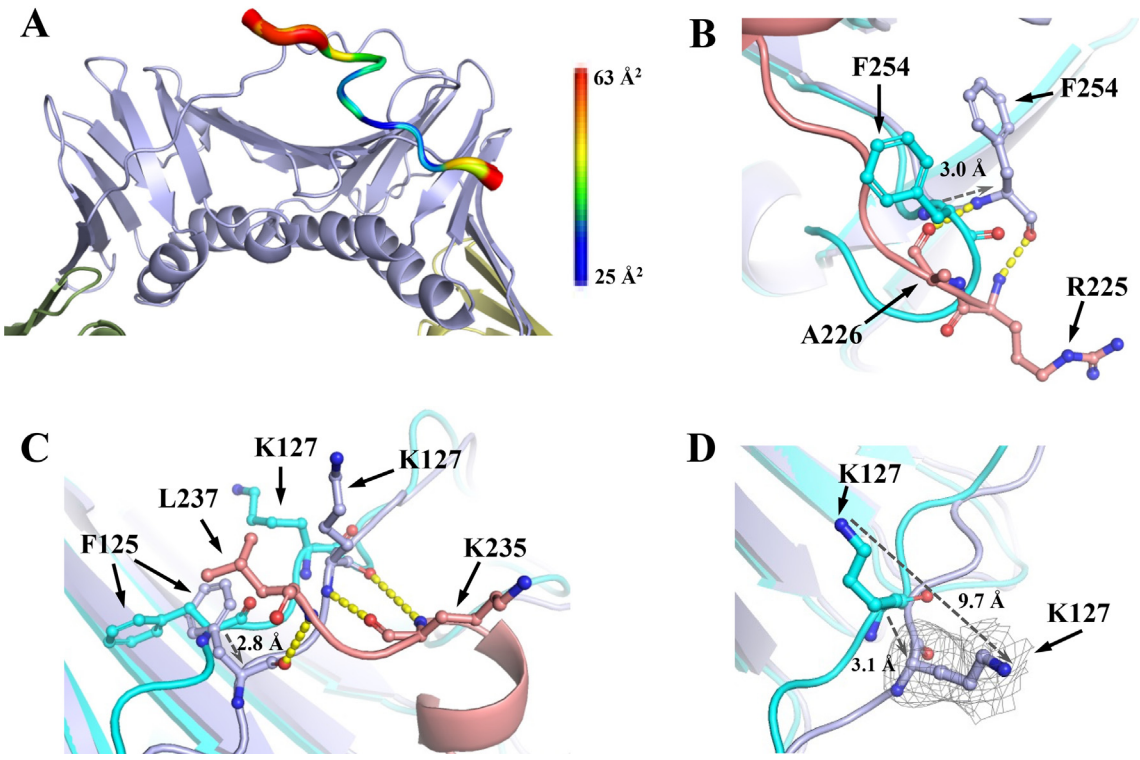

Figure 4. Interactions between PCNA and PIP flanking residues of CAF-1. (A) Alignment of the three PCNA monomers and three bound PIP motifs with B-factors for each PIP motif shown. Low B-factors are indicated in blue (thin tube) and high B-factors are indicated in red (thick tube). B-factor values are indicated by a color spectrum bar. (B) Close-up view of interactions between the N-terminal flanking PIP residues and the C-terminus of PCNA (bonds shown as yellow dashed lines). Cac1 residues (pink) interacting with F254 of PCNA (light purple). The position of F254 in the structure of unbound PCNA (PDB 1PLQ) is shown in cyan. The distance between the α-carbons of F254 in the unbound and PIP-bound PCNA structures is indicated by a dashed arrow. (C) Close-up view of interactions (yellow dashed lines) between the C-terminal flanking PIP residues and the IDCL of PCNA. The distance between the α-carbons of F125 in the unbound and PIP-bound PCNA structures is indicated by a dashed arrow. (D) Distance between positions of K127 in the unbound (cyan) and PIP-bound (light purple) structures of PCNA (indicated by dashed arrows). The Fo-Fc omit electron density map (shown as grey mesh) surrounding K127 in the PIP-bound structure was contoured at 2.0 σ.

observed in any monomer of our structure. This is likely due to R225 and A226 occupying the same space as these C-terminal residues of PCNA in the unbound, wildtype PCNA structure, causing a repositioning of these dynamic PCNA amino acids.

Density is present for three amino acids C-terminal to the PIP motif of CAF-1 (^{235}KKL^{237}). Two of the three amino acids interact with PCNA – K235 and L237. In contrast to the N-terminal residues R225 and A226, the polar interactions observed between PCNA and K235 or L237 are consistent among the three monomers. The first amino acid C-terminal to the PIP motif of CAF-1, K235, forms hydrogen bonds with the backbone of K127 on the IDCL of PCNA (Figure 4C). Due to this, the position of K127 (the α-carbon) is shifted between 2.7 and 3.1 Å closer to the bound PIP motif compared to the wildtype, unbound PCNA structure (PDB 1PLQ) in all three monomers (Figure 4D). Furthermore, the side chain of PCNA K127 resides in a drastically different location in the PIP-bound structure. The long side chain of the lysine typically points downward, toward the back surface of the PCNA molecule in the uncomplexed structure. Upon binding the PIP motif of CAF-1, this lysine is now rotated approximately 90° and pointing outward radially from the center of the PCNA molecule. Here, the ζ-nitrogen of the lysine is repositioned by 9.3–12.0 Å in all three monomers compared to the unbound PCNA structure (Figure 4D). The second amino acid C-terminal to the PIP motif of CAF-1, L237, interacts with the backbone of F125 in all three monomers, which is also located on the IDCL of PCNA. Due to this interaction, the α-carbon of F125 is shifted by a range of 2.6–2.8 Å in the different monomers, compared to the unbound structure of PCNA (Figure 4C).

Structural alignment of PIP motifs bound to PCNA in yeast

To the best of our knowledge, the structure of only two other canonical PIP motifs bound to PCNA in yeast have been solved, including those from the DNA ligase I (Cdc9, PDB: 2OD8) and the sliding clamp loader replication factor C (RFC, PDB: 1SXJ).[35,36] Cdc9 has a canonical PIP sequence (QATLARFF), while subunit 1 of RFC has a slightly less canonical PIP sequence where the first amino acid is an asparagine instead of a glutamine (NMSVVGYF). It should be noted that the entire RFC heteropentamer was present in the structure of RFC bound to PCNA.

An alignment of the PIP sequences and structures of the CAF-1, Cdc9, and RFC PIP motifs bound to PCNA are shown in Figure 5. As expected, the conserved residues within the PIP motif of all three yeast structures (Q/N1, h4, a7, and a8) bind to PCNA similarly, in the canonical manner in the PIP-binding region on PCNA (Figure 5B). The non-conserved PIP residues (positions 2, 3, 5, and 6) of these structures are also in similar positions (Figure 5C). However, positions of the amino acids flanking either side of the PIP motif are drastically different in all three structures (Figure 5D). In fact, the α-carbon of the residue in position $n = -2$ (two amino acids upstream of the first residue in the PIP motif) is shifted by as much as 10.8 Å, and the α-carbon of the residue in position $n = +2$ (two amino acids downstream of the last residue in the PIP motif) is shifted by as much as 10.0 Å (Figure 5E). No density was observed for amino acids downstream of the Cdc9 PIP sequence in the crystal structure. These differences, as well as the binding of the PIP motifs of CAF-1, Cdc9, or RFC, do not appear to cause any major structural differences within PCNA. The largest variations are observed within the IDCL. The RMSD value for PCNA monomers between the CAF-1 and Cdc9 structure was 0.370 Å, while the RMSD value for PCNA monomers between the CAF-1 and RFC structure was 0.581 Å (Figure 5F). These values are very low, even despite the difference in space groups of each crystal structure.

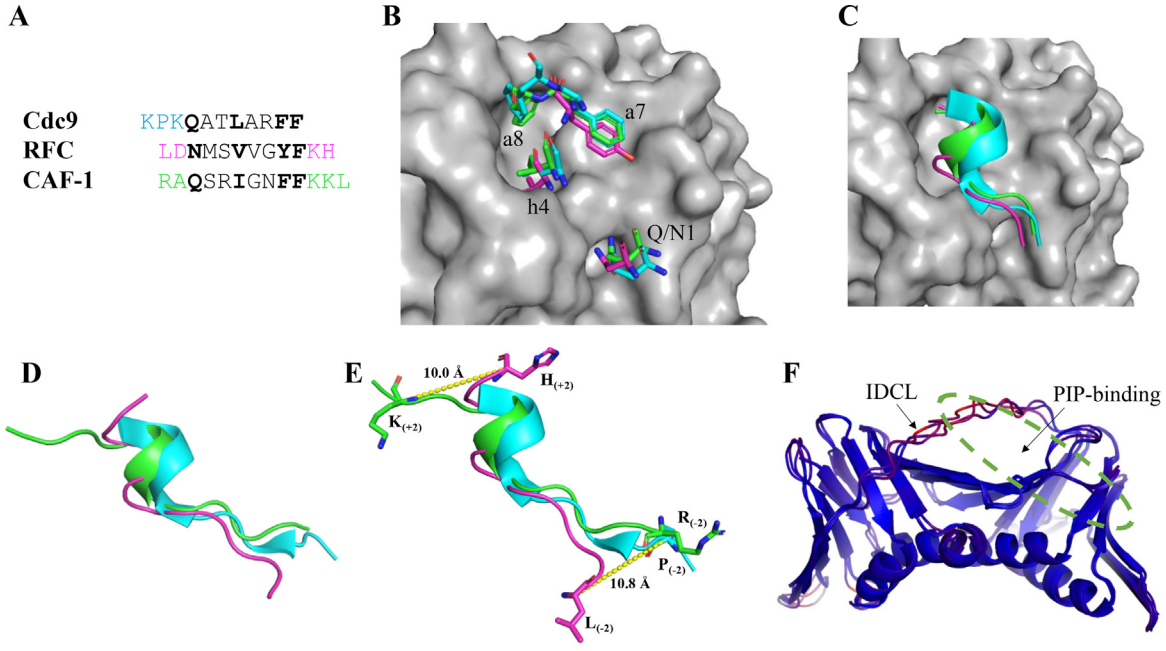

Figure 5. Comparison of PIP-bound PCNA structures in yeast. (A) Sequence alignment of the PIP motif of CAF-1 with the PIP motifs from Cdc9 and RFC (subunit 1). PIP residues are indicated in black (conserved residues are bolded) and flanking residues that were observed in each structure are indicated in color. (B) Positions of conserved residues – Q/N1, h4, a7, and a8 – within CAF-1 (green), Cdc9 (blue), and RFC (pink) PIP motifs, are shown bound to the PIP-binding pocket on PCNA (grey, surface). (C) Cartoon representation of structural alignment of the CAF-1, Cdc9, and RFC PIP motifs bound to PCNA (grey, surface). Only residues within the PIP sequences are shown. (D) Cartoon representation of the structures of the CAF-1, Cdc9, and RFC PIP motifs, including all observed flanking residues, bound to PCNA (PCNA not shown). (E) Distances between α-carbons of PIP-flanking residues within the CAF-1, Cdc9, and RFC PIP structures. PIP-flanking residues in the +2 or −2 positions in each structure are shown as sticks. (F) RMSD values between PCNA monomers of the CAF-1, Cdc9, and RFC PIP-bound structures represented by color. Structures of the PIP-bound PCNA proteins were overlaid and colored by a spectrum, indicating the minimum pairwise RMSD (blue) and maximum (red). Locations of the IDCL and PIP-binding pocket (green dashed line) on PCNA are labeled.

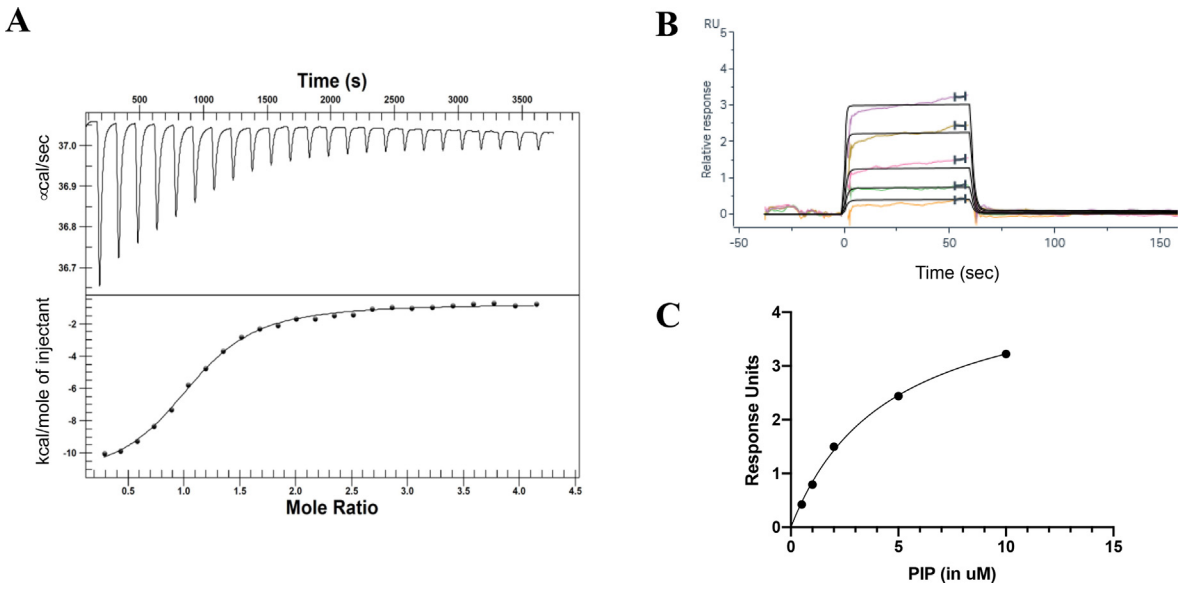

Figure 6. Thermodynamic and kinetic binding studies of the CAF-1 PIP motif and PCNA. (A) ITC of PCNA injected into a solution containing an isolated CAF-1 PIP peptide. The best fit of the data was used to determine thermodynamic binding parameters as $K_d = 3.54 \times 10^{-6} \pm 2.6 \times 10^{-7}$ M, $\Delta H = -10.9 \pm 0.15$ kcal/mol, $T\Delta S = -3.1 \pm 0.2$ kcal/mol, and a stoichiometry of 1.057 ± 0.007 (corresponding to PIP:PCNA monomer). (B) SPR of the isolated CAF-1 PIP peptide binding to immobilized PCNA. Concentrations of the PIP peptide at 0.5 (orange), 1.0 (green), 2.0 (pink), 5.0 (brown), and 10 μM (purple) were injected onto PCNA captured on the chip (top panel). Signal from injection of buffer only (no PIP peptide) was subtracted from all data. Resulting curves were fit to a two-step binding equation (BIAevaluation software). Kinetic values were measured as $1.37 \times 10^5 \pm 2.4 \times 10^3$ $M^{-1}sec^{-1}$ and $7.43 \times 10^{-1} \pm 1.3 \times 10^{-2}$ sec^{-1} for k_1 and k_{-1}, respectively, and $6.18 \times 10^{-4} \pm 2.6 \times 10^{-5}$ sec^{-1} and $1.67 \times 10^{-3} \pm 3.2 \times 10^{-4}$ sec^{-1} for k_2 and k_{-2}, respectively. These parameters resulted in a K_d of 3.96×10^{-6} M ± 9.1×10^{-7} M. The Chi^2 value was 0.008. (C) Responses at equilibrium for each concentration of PIP peptide were plotted and fit to a non-linear regression to obtain the steady state affinity of the interaction ($K_d = 3.98 \times 10^{-6}$ M ± 5.8×10^{-7} M). The χ^2 value was 0.003.

Thermodynamics and kinetics of the interaction between PCNA and CAF-1

Binding between the PIP motif of CAF-1 and PCNA was measured quantitatively using isothermal titration calorimetry (ITC) and surface plasmon resonance (SPR). For ITC, PCNA was injected into a sample cell containing the PIP motif of CAF-1 (residues 221–241). The thermodynamic parameters were measured as $K_d = 3.5 \pm 0.3$ μM, $\Delta H = -10.9 \pm 0.15$ kcal/mol, $T\Delta S = -3.1 \pm 0.2$ kcal/mol, and n = 1.06 ± 0.007 (corresponding to a stoichiometry of 1:1 for PCNA monomer:PIP motif) (Figure 6A). These results indicate the interaction is predominantly enthalpically-driven, which suggests interactions between the PIP of CAF-1 and PCNA are slightly more hydrophilic than hydrophobic.

For SPR experiments, PCNA was captured on the surface of a sensor chip and increasing concentrations of the PIP peptide (residues 221–241) were added to the chip (Figure 6B). The binding affinity of the PCNA-CAF-1 interaction, obtained by plotting the steady state response units vs ligand concentration, was $K_d = 4.0 \pm 0.6$ μ M (Figure 6C). This is in close agreement to the dissociation constant determined from ITC experiments and is similar to many other PCNA-PIP interactions that occur during DNA replication and repair, as described previously.[37,38] Evaluation of SPR results revealed a two-step binding mechanism. Kinetic rate constants were determined to be $1.37 \times 10^5 \pm 2.4 \times 10^3$ $M^{-1}sec^{-1}$ and $7.43 \times 10^{-1} \pm 1.3 \times 10^{-2}$ sec^{-1} for k_1 and k_{-1}, respectively, and $6.18 \times 10^{-4} \pm 2.6 \times 10^{-5}$ sec^{-1} and $1.67 \times 10^{-3} \pm 3.2 \times 10^{-4}$ sec^{-1} for k_2 and k_{-2}, respectively, suggesting association of the first step is relatively fast, which is followed by a much slower step involving a conformational change. These rate constants also correspond to a K_d of 4.0 ± 0.9 μM, in agreement with the steady state dissociation constant obtained from Figure 6C.

PIP-flanking residues are important for the affinity of CAF-1 for PCNA in vitro

The sequence of the CAF-1 PIP motif is highly conserved amongst yeast species (Figure 7A). Interestingly, there are several charged residues flanking the PIP motif, both N-terminally and C-terminally, that are also completely conserved within these species. To determine the importance

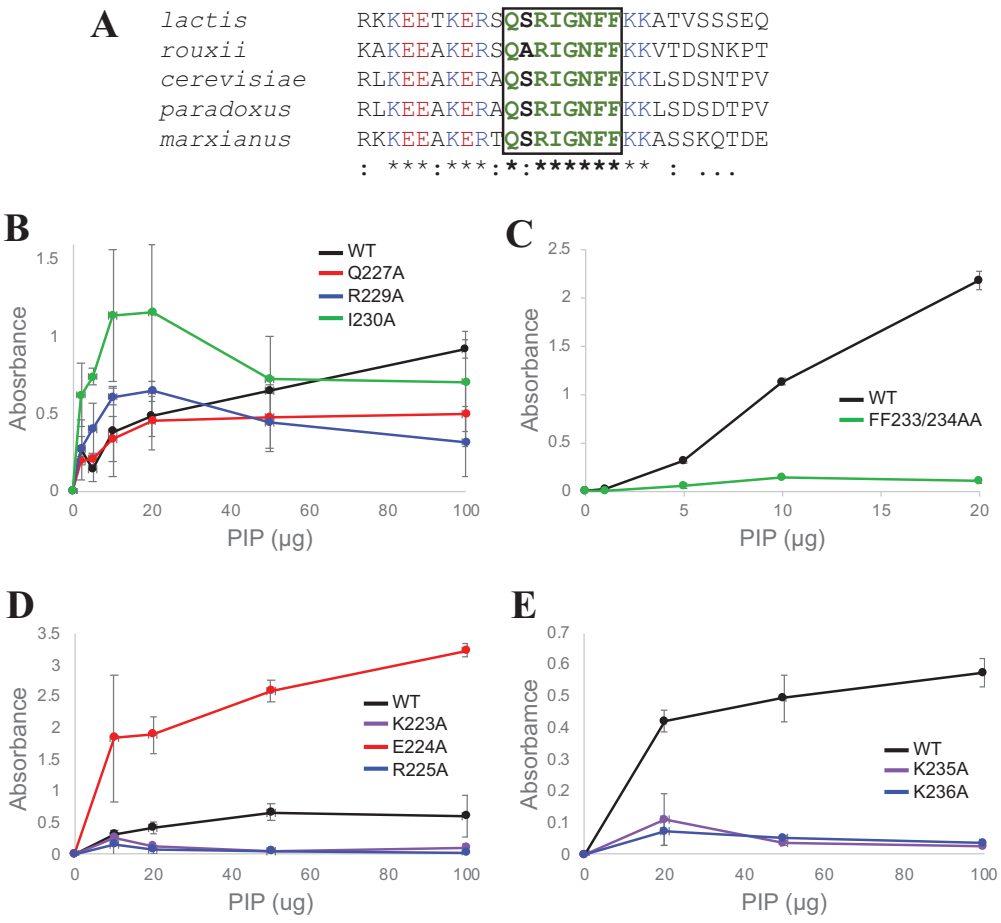

Figure 7. Positive charges flanking the PIP motif of yeast CAF-1 are important for PCNA binding affinity. (A) Sequence alignment of the PIP and surrounding residues in various yeast species. Positive (blue) and negative (red) conserved PIP-flanking residues are indicated by an asterisk. Conserved PIP motif residues (green, boxed) are also indicated by an asterisk. (B) ELISA of PCNA binding to wildtype or mutant CAF-1 PIP peptides containing substitutions within the PIP sequence. Wildtype, biotinylated PIP peptide (residues 221–241) (black) or peptides containing a Q227A (red), R229A (blue), or I230A (green) substitution were added to wells containing PCNA and detected using anti-biotin. (C) ELISA of PCNA binding to the wildtype CAF-1 PIP peptide (black) or the PIP peptide containing a FF233/234AA (green) double substitution. (D) ELISA of PCNA binding to wildtype or mutant CAF-1 PIP peptides containing substitutions upstream of the PIP sequence. Wildtype PIP peptide (black) or peptides containing a K223A (purple), E224A (red), or R225 (blue) substitution were added to wells containing PCNA. (E) ELISA of PCNA binding to wildtype or mutant CAF-1 PIP peptides containing substitutions downstream of the PIP sequence. Wildtype PIP peptide (black) or peptides containing a K235A (purple), or K236A (blue) substitution were added to wells containing PCNA.

of these conserved residues within and surrounding the PIP motif of CAF-1 in binding PCNA, we carried out enzyme-linked immunosorbent assays (ELISAs) using CAF-1 PIP peptides (residues 221–241) containing alanine mutations, as shown in Table 2. Here, PCNA was attached to the bottom of a well in a 96-well plate and increasing amounts of wildtype or mutant, biotinylated CAF-1 PIP peptides were added. The relative amount of PIP peptide bound to PCNA in each well was measured using a biotin antibody.

We first carried out ELISAs with PIP peptides containing alanine substitutions within the PIP motif itself, including the conserved amino acids Q227A, R229A, and I230A (Figure 7B). Results showed mutations in any one of these residues did not significantly inhibit the interaction with PCNA, suggesting the conserved glutamine, arginine, and isoleucine residues in the PIP motif of yeast CAF-1 proteins are not critical for specific binding to PCNA. As expected, binding between the CAF-1 peptide and PCNA was almost

Table 2 Wildtype and mutated PIP peptides used in ELISA studies.

Substitution	Peptide Sequence
Wildtype	WEAKERAQSRIGNFFKKLSDSNT
K223A	WEAAERAQSRIGNFFKKLSDSNT
E224A	WEAKARAQSRIGNFFKKLSDSNT
R225A	WEAKEAAQSRIGNFFKKLSDSNT
Q227A	*WEAKERAASRIGNFFKKLSDSNT*
R229A	*WEAKERAQSAIGNFFKKLSDSNT*
I230A	*WEAKERAQSRAGNFFKKLSDSNT*
FF233/234AA	*WEAKERAQSRIGNAAKKLSDSNT*
K235A	WEAKERAQSRIGNFFAKLSDSNT
K236A	WEAKERAQSRIGNFFKALSDSNT

Italicized residues represent those within the PIP motif. Red residues indicate mutations.

completely inhibited when the two conserved phenylalanine residues within the PIP motif were mutated to alanine simultaneously (Figure 7C). This specific mutation in canonical PIP motifs inhibits binding to PCNA.[36,39–41]

Next, we measured the importance of several conserved residues immediately upstream or downstream of the PIP motif on the interaction between PCNA and CAF-1. When two of the positively charged amino acids N-terminally flanking the PIP were mutated to alanine (K223A or R225A), binding to PCNA was reduced compared to the wildtype PIP peptide (Figure 7D). Similar results were observed when either of the two positively charged lysine residues immediately C-terminal to the PIP motif were substituted with alanines, where the K235A and K236A mutant PIP peptides bound PCNA with lower affinity than wildtype (Figure 7E). The opposite effect was observed for the negatively charged E224 residue, as the E224A mutant PIP peptide bound PCNA significantly tighter than the wildtype PIP peptide (Figure 7D). These results validate the thermodynamic data described above, which also suggest the interaction between the PIP motif of CAF-1 and PCNA is more hydrophilic in nature. Together, these results suggest that, not only are the residues flanking the PIP motif of CAF-1 more crucial for specific binding to PCNA than residues within the PIP motif itself, but charged residues – specifically those with positively charged side chains – are essential for the interaction between CAF-1 and PCNA *in vitro*.

Expression of mutant CAF-1 proteins affect gene silencing to differing extents in vivo

Finally, we set out to determine the effect of the above amino acid mutations within and surrounding the PIP motif of CAF-1 on gene silencing *in vivo*. We measured silencing by Cac1 at the *HMR* locus using yeast cells containing the gene for GFP in place of the *HMR* locus and lacking the gene for endogenous Cac1 (*cac*1Δ). These cells thus expressed GFP, as CAF-1 was unable to silence its expression (Figure 8). Quantification of GFP expression was determined using flow cytometry. Upon transformation of a plasmid containing the gene for Cac1 expression, GFP silencing was rescued. We next transformed *cac*1Δ cells with an expression plasmid containing a mutant form of the gene encoding Cac1 (K223A, E224A, R225A, R229A, I230A, FF233/234AA, K235A, or K236A) to determine whether these mutant CAF-1 proteins could also rescue GFP silencing. Results showed all the mutant proteins either partially or fully restored silencing compared to the empty vector or when no plasmid was transformed into the cells.

Discussion

PCNA is an essential player in DNA metabolism, where it interacts with and regulates the activities of a plethora of interacting partners during a variety of DNA-templated processes. These PCNA-interacting proteins typically contain a PIP motif that binds in a hydrophobic pocket on the front face of PCNA between its C-terminus and the IDCL. Precisely how this replication accessory protein can discriminate between a multitude of binding partners to coordinate their access to and function on DNA using a motif of only eight amino acids – and often only four of these residues are variable – is still unclear. It is becoming more apparent that residues immediately upstream and/or downstream of the PIP motif are important for specificity and affinity of their interaction with PCNA. For example, p21, a cyclin-dependent kinase inhibitor, contains a PIP motif with the highest known affinity to PCNA (~80—500 n M).[37,42] This high affinity is due to an extensive number of interactions with PCNA and amino acids

flanking the PIP motif, where both N-terminal and C-terminal residues form anti-parallel β-sheets with the C-terminus of PCNA and the IDCL of PCNA, respectively.[28] Residues flanking both ends of the PIP motif in the flap endonuclease 1 (FEN1) also contact the IDCL and C-terminus of PCNA, but to a lesser extent than p21.[29] Residues C-terminal to the PIP motif of polymerase eta, a translesion synthesis polymerase, contact the IDCL of PCNA, but with an even fewer number of interactions than observed in either p21 or FEN1.[43] The number of interactions between polymerase eta and PCNA, however, are more extensive than those observed for other translesion synthesis polymerases, polymerase kappa and polymerase iota. Although composed of five subunits, the PCNA clamp-loading complex, replication factor C (RFC), has only one canonical PIP motif (within subunit 1), which interacts with the C-terminus of PCNA via residues N-terminally flanking its PIP motif.[35] Finally, the yeast DNA ligase Cdc9 interacts with PCNA via residues N-terminal to its PIP motif by forming a short, antiparallel β-sheet with the C-terminus of PCNA.[36]

The direct interaction between PCNA and CAF-1 is required for normal nucleosome assembly and gene silencing.[13,16,17,24,26] To understand the structural mechanism of binding between PCNA and CAF-1 and how it might differ from other PCNA-PIP interactions, we solved the structure of the PIP motif of CAF-1 bound to PCNA. As expected, the four conserved residues (Q1, I4, F7, and F8) of the CAF-1 PIP motif bound to PCNA in a manner very similar to other canonical PIP motifs, whereas the non-conserved residues in the PIP motif (S2, R3, G5, N6) formed interactions with PCNA that were similar to, but slightly variable from other canonical PIP motifs. For instance, the backbone nitrogen in S2 of the CAF-1 PIP motif forms a hydrogen bond with the backbone carboxyl of P252 in PCNA. Although the amino acid in position 2 of the Cdc9 PIP motif is an alanine, its backbone nitrogen also interacts with the carboxyl of P252 in PCNA. Moreover, the sidechains of S2 and R3 in the CAF-1 PIP motif make contacts with the backbone carboxyl groups of P252 and S43 in PCNA, respectively. Conversely, the side chains of the second and third amino acids in the Cdc9 PIP motif, alanine and threonine, respectively, do not form additional contacts with PCNA. In addition to residues of the CAF-1 PIP motif itself, we observed density for amino acids flanking either side of the motif and interactions between these residues and PCNA. Similar to p21 and FEN1, residues N-terminal to the PIP motif of CAF-1 interact with the C-terminus of PCNA and residues C-terminal to the PIP motif of CAF-1 interact with the IDCL of PCNA. However, these contacts between CAF-1 and PCNA are not as extensive as those formed between PCNA and p21 or FEN1.

Contrary to expectation, the number of interactions formed between PCNA and PIP-flanking residues in these proteins does not

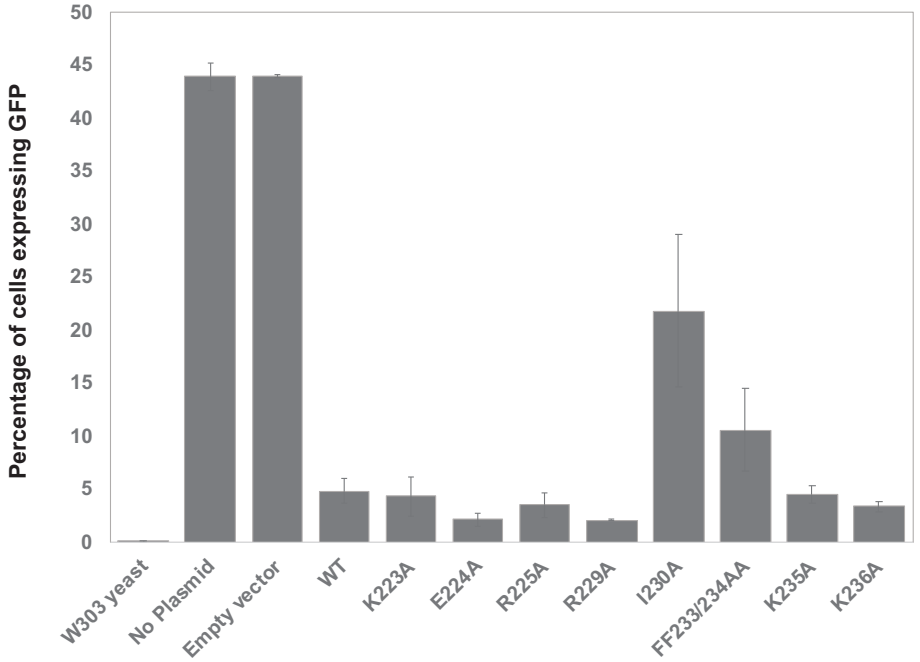

Figure 8. Effects of mutant CAF-1 proteins on gene silencing. Silencing of GFP by wildtype (WT) or mutant Cac1 proteins was measured by flow cytometry. Non-GFP-expressing yeast cells (W303), untransformed GFP-expressing yeast cells (no plasmid), and GFP-expressing yeast cells containing the pRS313 vector only (empty vector) were used as controls. Error bars represent the standard error of the mean from two replications of the experiment.

always correlate with affinity. The majority of PIP motifs studied thus far, in both yeast and humans, exhibit affinities toward PCNA on the micromolar scale, typically between 1 and 60 μM.[37,38] As mentioned above, the PIP motif of p21 has the highest affinity for PCNA, which is in the sub-micromolar range (~80–500 nM).[42,44,45] The PIP motif of FEN1, although making extensive contacts with PCNA using residues both N-terminal and C-terminal to the motif, has the lowest known affinity for PCNA, upwards of 60 μM.[42] Polymerase eta, which only makes additional contacts to PCNA using amino acids C-terminal to the PIP motif – and these contacts are less in number than those observed between FEN1 and PCNA – has the second-highest known affinity for PCNA (~0.4 μM).[43] Here, we determined the affinity between PCNA and the PIP motif of CAF-1 to be ~4.0 μM. This is within the typical range of PCNA-PIP interactions and may be close to the expected value due to additional yet non-extensive interactions with PCNA using residues flanking both sides of the PIP motif.

It is important to note the structure of a human CAF-1 PIP motif bound to PCNA was recently published.[46] In humans, the largest, PIP-containing subunit of CAF-1 is called p150. The structure showed the PIP motif of p150 bound to PCNA in a manner distinct from any PIP-PCNA interaction observed previously. The PIP motif bound in the canonical PIP-binding hydrophobic pocket in PCNA but was oriented almost perpendicular to the pocket. It appeared to form a cation-π interaction with PCNA, also unlike any other PIP-PCNA interaction whose structure has previously been determined. Based on these and our results, it is possible that the PIP motifs of human and yeast CAF-1 bind PCNA via different mechanisms. In support of this, the sequences of the human and yeast CAF-1 PIP motifs are quite different (the human sequence is KAEITRFF). Human CAF-1 contains two PIP motifs, called PIP1 and PIP2. These two motifs are located rather far from each other within the primary sequence of p150, where PIP1 is near the N-terminus and PIP2 is close to the center of the subunit.[47] The human PIP-PCNA structure determined was of the PIP2 motif, whereas the PIP1 has an even more unconventional sequence (QARLPF). Therefore, it is possible this PIP motif in yeast CAF-1 more resembles that of the PIP1 in humans in terms of binding PCNA; however, the location and sequence of the yeast PIP motif CAF-1 is much more similar to that of the PIP2 motif in humans. In fact, the affinity of the yeast Cac1 PIP motif to PCNA measured here is the same as that measured for the human PIP2 (5.4 μM).[47] Finally, in the human PIP-PCNA crystal structure, density was only observed for the last three amino acids in the motif (R6, F7, F8). Thus, it is possible that the atypical PIP-PCNA interaction observed with the human p150 motif may be a non-physiological mode of interaction, or it represents one of multiple binding mechanisms between CAF-1 and PCNA.

Similar to previous studies using other PIP-containing proteins, our data demonstrate amino acids flanking the PIP motif in CAF-1 are required for specificity and affinity of binding to PCNA. In addition, PIP motifs surrounded by positively charged amino acids tend to display increased affinity for PCNA, whereas a negative charge upstream of the CAF-1 PIP motif prevents an even tighter interaction with PCNA. Together, these studies suggest positive charges flanking the PIP motif are necessary for a high affinity interaction with PCNA, but the specific types of bonds formed and residues involved in the interaction – both within the PIP motif and within PCNA – can be quite variable. Several pieces of evidence support this. First, even though PIP-flanking residues are clearly important for PCNA-binding specificity and affinity, their interactions with PCNA tend to be more dynamic than residues within the PIP motifs themselves. Based on numerous structures of PIP motifs bound to PCNA, B-factors of PIP-flanking residues in these structures are much higher than residues within the PIPs themselves (Figure 9). This may be expected since the flanking residues are at the "ends" of the PCNA-binding sequence in each structure, which typically have more flexibility in protein structures. However, these residues also have larger B-factors in a structure containing full-length proteins bound to PCNA (such as RFC) and structures that truncate at the N- or C-terminus of the PIP motif sequence do not show variability at the "ends" (the Cdc9 structure truncates at F8 – which shows low B-factors – and structures of polymerases iota and kappa truncate at K1 – which show low B-factors). Interestingly, there appears to be a trend of higher flexibility in positively charged residues of these flanking regions. Amino acids C-terminally flanking the PIP motifs of p21 (HSKRRLIFS) and polymerase eta (KPLT) are the outliers to this trend; however, these two proteins have the two highest recorded affinities for PCNA, and these residues have been demonstrated to confer the tight binding of these proteins for PCNA.[37,42,43] Second, the asymmetric unit for the crystal structure of the CAF-1 PIP motif bound to PCNA described here revealed three PIP motifs of CAF-1 bound to three PCNA monomers. Residues within the PIP motif were all in very similar positions, but flanking residues made slightly different polar interactions with each monomer of PCNA. This is also observed in the structures of other PIP motifs bound to PCNA where more than one PCNA monomer was present in the asymmetric unit. In the case of the structures of the polymerase eta, iota, or kappa PIP motif bound to PCNA, the contacts made

with the different monomers of PCNA in each structure are even more variable (see PDBs 2ZVK, 2ZVL, and 2ZVM).

If the specific type of bonds made within a PCNA-PIP interaction is not crucial, there are other possibilities regarding the significance of the specific flanking residues. First, the surface of PCNA is rather negatively charged – both near the PIP-binding pocket and throughout the entire surface of the protein. Therefore, multiple interactions may be possible between positive charges near PIP motifs and the surface of PCNA, and thus there is flexibility as to the specific contacts made between the two proteins. This would also help PCNA discriminate between binding partners. The PIP-flanking residues in PCNA-binding proteins may fine tune their affinities with PCNA, whether these residues increase the affinity (via positively charged side chains) or decrease it (via negatively charged side chains). Alternatively, certain flanking side chains may position PIP residues to form more efficient interactions with PCNA. This sort of scenario was observed when C-terminal flanking residues of the polymerase kappa PIP motif were replaced with those of polymerase eta (PLTH). This substitution increased the affinity of polymerase kappa for PCNA, but the PLTH residues themselves did not appear to form any contacts with PCNA.[43] Ultimately, it seems affinity and specificity of PCNA-PIP interactions cannot be predicted by sequence alone but require independent structural and quantitative measurements.

Complementary assays were carried out to examine the relationship between the interaction of CAF-1 and PCNA *in vitro* and the function of CAF-1 *in vivo*. Interestingly, results showed no direct correlation between the two. These data suggest the relationship between the structural interaction of CAF-1 and PCNA and the gene silencing function of CAF-1 in the cell is not straightforward. This is expected, however, as replication-coupled nucleosome assembly and subsequent gene silencing involve multiple, dynamic complexes composed of numerous protein factors and DNA substrates. To this point, previous studies in both human and yeast cells have also shown non-PCNA binding CAF-1 mutants do not inhibit gene silencing significantly *in vivo*.[24,47] Together, these results suggest CAF-

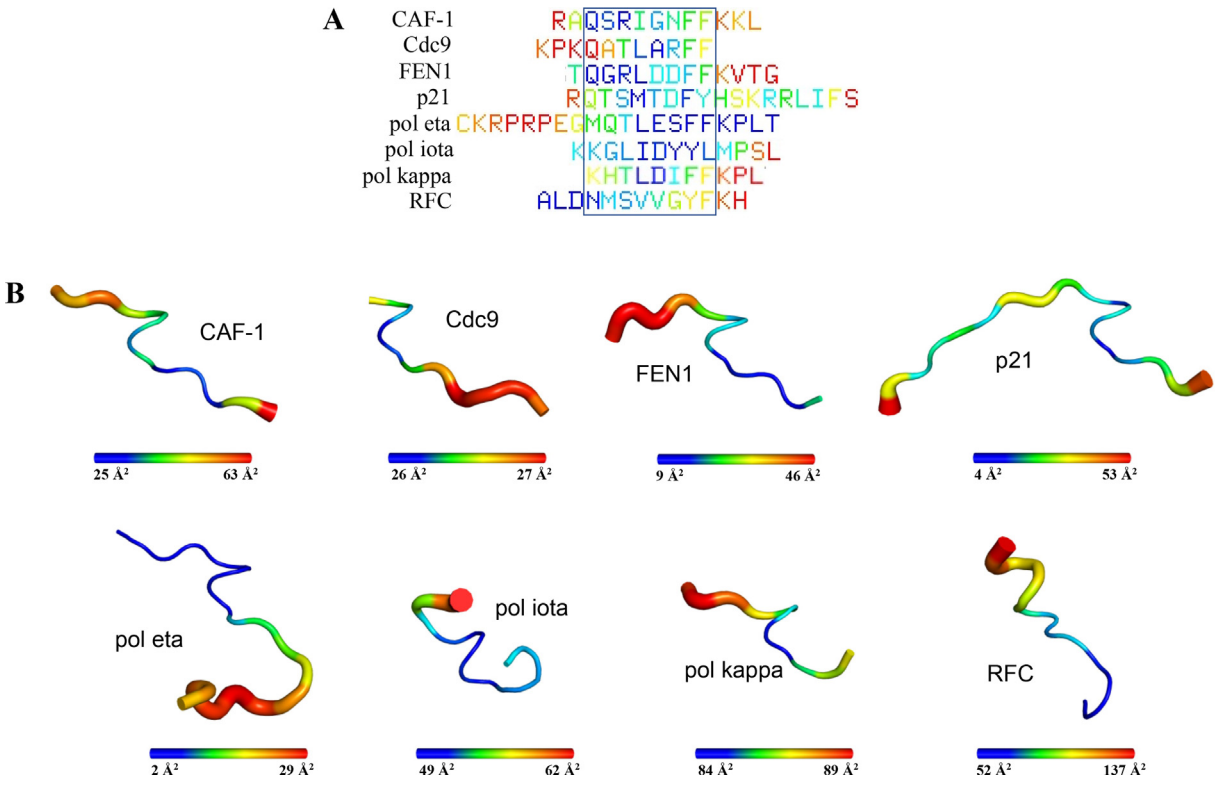

Figure 9. B-factors within PIP motif sequences upon binding to PCNA. (A) Sequence alignment of PIP and flanking residues observed within structures of various PIP peptides bound to PCNA. Low B-factors are indicated in blue and high B-factors are indicated in red. PIP residues are boxed. (B) B-factors of PIP peptides from various PCNA-binding proteins upon binding PCNA. Structures are from the following PDB codes: Cdc9 (PDB 2OD8), FEN1 (PDB 1U7B), p21 (PDB 1ACX), pol eta (PDB 2ZVK), pol iota (PDB 2ZVM), pol kappa (PDB 2ZVL), and RFC (PDB 1SXJ). Low B-factors are indicated in blue (thin tube) and high B-factors are indicated in red (thick tube). B-factor values are indicated below each structure by a color spectrum bar.

1 is making contacts with other factors in the cell, such as DNA or other proteins involved in gene silencing, and these interactions may be compensating for weaker PCNA interactions. In our studies, two mutant Cac1 proteins, I230A and FF233/234AA, exhibited decreased silencing compared to wildtype Cac1. These specific mutations may impair the ability of CAF-1 or the CAF-1-PCNA complex to adopt the fully active conformational state required for proper gene silencing. Future work is needed to examine these possibilities and dissect the precise mechanism of CAF-1-mediated gene silencing *in vivo*.

CRediT authorship contribution statement

Keely S. Orndorff: Formal analysis, Investigation. **Evan J. Veltri:** Formal analysis. **Nicole M. Hoitsma:** Formal analysis, Investigation, Writing – review & editing. **Ivy L. Williams:** Formal analysis, Investigation. **Ian Hall:** Formal analysis, Investigation, Writing – review & editing. **Grace E. Jaworski:** Formal analysis, Investigation, Writing – review & editing. **Grace E. Majeres:** Investigation. **Samaya Kallepalli:** Investigation. **Abigayle F. Vito:** Investigation. **Lucas R. Struble:** Resources. **Gloria E.O. Borgstahl:** Resources. **Lynne M. Dieckman:** Conceptualization, Formal analysis, Funding acquisition, Methodology, Supervision, Writing – original draft.

DECLARATION OF COMPETING INTEREST

The authors declare that they have no known competing financial interests or personal relationships that could have appeared to influence the work reported in this paper.

Acknowledgements

We would like to thank Dr. Bret Freudenthal at the University of Kansas Medical Center for resources and assistance in collecting the X-ray crystallography data. We thank Dr. Bruce Stillman at Cold Spring Harbor Laboratory for providing yeast strains and plasmids for the gene silencing assays. We thank Dr. Omalla Olwenyi and the Flow Cytometry Shared Resource at Creighton University for assistance with flow cytometry experiments and analysis. We thank Dr. M. Todd Washington for valuable discussions. We thank Jeffrey Lovelace for technical assistance. The project described was supported by Award Number 2047553 from the National Science Foundation and Award Number P20GM103427 from the National Institutes of Health to L.M.D. Support was also provided by the Fred and Pamela Buffett NCI Cancer Center Support Grant (P30CA036727) to G.E.O.B. NMH is a Howard Hughes Medical Institute Fellow of the Damon Runyon Cancer Research Foundation, DRG-2499-23. The content is solely the responsibility of the authors and does not necessarily represent the official views of the National Science Foundation or the National Institutes of Health.

Received 9 November 2023;
Accepted 1 July 2024;
Available online 04 July 2024

Keywords:
Chromatin assembly factor 1;
Proliferating cell nuclear antigen;
Nucleosome assembly;
PCNA-interacting peptide (PIP);
Gene silencing

References

1. Maga, G., Hubscher, U., (2003). Proliferating cell nuclear antigen (PCNA): a dancer with many partners. *J. Cell Sci.* **116**, 3051–3060.
2. Moldovan, G.L., Pfander, B., Jentsch, S., (2007). PCNA, the Maestro of the Replication Fork. *Cell*.
3. Naryzhny, S.N., (2008). Proliferating cell nuclear antigen: a proteomics view. *Cell. Mol. Life Sci.* **65**, 3789–3808.
4. Tsurimoto, T., (1999). PCNA binding proteins. *Front. Biosci.* **4**, d849
5. Zhuang, Z., Ai, Y., (2010). Processivity factor of DNA polymerase and its expanding role in normal and translesion DNA synthesis. *BBA* **1804**, 1081–1093.
6. Dieckman, L.M., Freudenthal, B.D., Washington, M.T., (2012). PCNA structure and function: insights from structures of PCNA complexes and post-translationally modified PCNA. *Subcell. Biochem.* **62**, 281–299.
7. Biasio, A.D., Blanco, F.J., (2013). Proliferating cell nuclear antigen structure and interactions. Elsevier, pp. 1–36.
8. Krishna, T.S.R., Kong, X.-P., Gary, S., Burgers, P.M., Kuriyan, J., (1994). Crystal structure of the eukaryotic DNA polymerase processivity factor PCNA. *Cell* **79**, 1233–1243.
9. Jonsson, Z.O., Hindges, R., Hubscher, U., (1998). Regulation of DNA replication and repair proteins through interaction with the front side of proliferating cell nuclear antigen. *EMBO J.* **17**, 2412–2425.
10. Burgess, R.J., Zhang, Z., (2013). Histone chaperones in nucleosome assembly and human disease. *Nature Struct. Mol. Biol.* **20**, 14–22.
11. Houlard, M., Berlivet, S., Probst, A.V., Quivy, J.P., Héry, P., Almouzni, G., Gérard, M., (2006). CAF-1 is essential for heterochromatin organization in pluripotent embryonic cells. *PLoS Genet.* **2**, e181.
12. Takami, Y., Ono, T., Fukagawa, T., Shibahara, K., Nakayama, T., (2007). Essential role of chromatin assembly factor-1–mediated rapid nucleosome assembly for DNA replication and cell division in vertebrate cells. *Mol. Biol. Cell* **18**, 129–141.
13. Quivy, J.P., Gérard, A., Cook, A.J.L., Roche, D., Almouzni, G., (2008). The HP1–p150/CAF-1 interaction is required for

pericentric heterochromatin replication and S-phase progression in mouse cells. *Nature Struct. Mol. Biol.* **15**, 972–979.
14. Klapholz, B., Dietrich, B.H., Schaffner, C., Hérédia, F., Quivy, J.P., Almouzni, G., Dostatni, N., (2009). CAF-1 is required for efficient replication of euchromatic DNA in Drosophila larval endocycling cells. *Chromosoma* **118**, 235–248.
15. Shibahara, K., Stillman, B., (1999). Replication-dependent marking of DNA by PCNA facilitates CAF-1-coupled inheritance of chromatin. *Cell* **96**, 575–585.
16. Moggs, J.G., Grandi, P., Quivy, J.P., Jonsson, Z.O., Hubscher, U., Becker, P.B., Almouzni, G., (2000). A CAF-1-PCNA-mediated chromatin assembly pathway triggered by sensing DNA damage. *Mol. Cell. Biol.* **20**, 1206–1218.
17. Stillman, B., Zhang, Z., Shibahara, K., (2000). PCNA connects DNA replication to epigenetic inheritance in yeast. *Nature* **408**, 221–225.
18. Kondratick, C.M., Litman, J.M., Shaffer, K.V., Washington, M.T., Dieckman, L.M., (2018). Crystal structures of PCNA mutant proteins defective in gene silencing suggest a novel interaction site on the front face of the PCNA ring. *PLoS One* **13**, e0193333.
19. Sauer, P.V., Timm, J., Liu, D., Sitbon, D., Boeri-Erba, E., Velours, C., Mücke, N., Langowski, J., Ochsenbein, F., Almouzni, G., Panne, D., (2017). Insights into the molecular architecture and histone H3–H4 deposition mechanism of yeast Chromatin assembly factor 1. *Elife* **6**
20. Zhang, K., Gao, Y., Li, J., Burgess, R., Han, J., Liang, H., Zhang, Z., Liu, Y., (2016). A DNA binding winged helix domain in CAF-1 functions with PCNA to stabilize CAF-1 at replication forks. *Nucleic Acids Res.*, gkw106.
21. Sauer, P.V., Gu, Y., Liu, W.H., Mattiroli, F., Panne, D., Luger, K., Churchill, M.E., (2018). Mechanistic insights into histone deposition and nucleosome assembly by the chromatin assembly factor-1. *Nucleic Acids Res.* **46**, 9907–9917.
22. Mattiroli, F., Gu, Y., Balsbaugh, J.L., Ahn, N.G., Luger, K., (2017). The Cac2 subunit is essential for productive histone binding and nucleosome assembly in CAF-1. *Sci. Rep.* **7**, 46274.
23. Mattiroli, F., Gu, Y., Yadav, T., Balsbaugh, J.L., Harris, M. R., Findlay, E.S., Liu, Y., Radebaugh, C.A., Stargell, L.A., Ahn, N.G., Whitehouse, L., Luger, K., (2017). DNA-mediated association of two histone-bound complexes of yeast Chromatin Assembly Factor-1 (CAF-1) drives tetrasome assembly in the wake of DNA replication. *Elife* **6**
24. Krawitz, D.C., Kama, T., Kaufman, P.D., (2002). Chromatin assembly factor I mutants defective for PCNA binding require Asf1/Hir proteins for silencing. *Mol. Cell. Biol.* **22**, 614–625.
25. Moggs, J.G., Grandi, P., Quivy, J.-P., Jónsson, Z.O., Hübscher, U., Becker, P.B., Almouzni, G., (2000). A CAF-1–PCNA-mediated chromatin assembly pathway triggered by sensing DNA damage. *Mol. Cell Biol.* **20**, 1206–1218.
26. Sharp, J.A., Fouts, E.T., Krawitz, D.C., Kaufman, P.D., (2001). Yeast histone deposition protein Asf1p requires Hir proteins and PCNA for heterochromatic silencing. *Curr. Biol.* **11**, 463–473.
27. Dieckman, L., (2020). Something's gotta give: How PCNA alters its structure in response to mutations and the implications on cellular processes. *Prog. Biophys. Mol. Biol.* **163**, 46–59.
28. Gulbis, J.M., Kelman, Z., Hurwitz, J., O'Donnell, M., Kuriyan, J., (1996). Structure of the C-terminal region of p21(WAF1/CIP1) complexed with human PCNA. *Cell* **87**, 297–306.
29. Sakurai, S., Kitano, K., Yamaguchi, H., Hamada, K., Okada, K., Fukuda, K., Uchida, M., Ohtsuka, E., Morioka, H., Hakoshima, T., (2005). Structural basis for recruitment of human flap endonuclease 1 to PCNA. *EMBO J.* **24**, 683–693.
30. Freudenthal, B.D., Ramaswamy, S., Hingorani, M.M., Washington, M.T., (2008). Structure of a mutant form of proliferating cell nuclear antigen that blocks translesion DNA synthesis. *Biochemistry* **47**, 13354–13361.
31. Adams, P.D., Afonine, P.V., Bunkóczi, G., Chen, V.B., Davis, I.W., Echols, N., Headd, J.J., Hung, L.-W., Kapral, G.J., Grosse-Kunstleve, R.W., McCoy, A.J., Moriarty, N. W., Oeffner, R., Read, R.J., Richardson, D.C., Richardson, J.S., Terwilliger, T.C., Zwart, P.H., (2010). PHENIX: a comprehensive Python-based system for macromolecular structure solution. *Acta Crystallogr. Sect. D Biol. Crystallogr.* **66**, 213–221.
32. Emsley, P., Cowtan, K., (2004). Coot: model-building tools for molecular graphics. *Acta Crystallogr. Sect. D Biol. Crystallogr.* **60**, 2126–2132.
33. Jumper, J., Evans, R., Pritzel, A., Green, T., Figurnov, M., Ronneberger, O., Tunyasuvunakool, K., Bates, R., Žídek, A., Potapenko, A., Bridgland, A., Meyer, C., Kohl, S.A.A., Ballard, A.J., Cowie, A., Romera-Paredes, B., Nikolov, S., Jain, R., Adler, J., Back, T., Petersen, S., Reiman, D., Clancy, E., Zielinski, M., Steinegger, M., Pacholska, M., Berghammer, T., Bodenstein, S., Silver, D., Vinyals, O., Senior, A.W., Kavukcuoglu, K., Kohli, P., Hassabis, D., (2021). Highly accurate protein structure prediction with AlphaFold. *Nature* **596**, 583–589.
34. Mirdita, M., Schütze, K., Moriwaki, Y., Heo, L., Ovchinnikov, S., Steinegger, M., (2022). ColabFold: making protein folding accessible to all. *Nature Methods* **19**, 679–682.
35. Bowman, G.D., O'Donnell, M., Kuriyan, J., (2004). Structural analysis of a eukaryotic sliding DNA clamp|[ndash]|clamp loader complex. *Nature* **429**, 724–730.
36. Vijayakumar, S., Chapados, B.R., Schmidt, K.H., Kolodner, R.D., Tainer, J.A., Tomkinson, A.E., (2007). The C-terminal domain of yeast PCNA is required for physical and functional interactions with Cdc9 DNA ligase. *Nucleic Acids Res.* **35**, 1624–1637.
37. Prestel, A., Wichmann, N., Martins, J.M., Marabini, R., Kassem, N., Broendum, S.S., Otterlei, M., Nielsen, O., Willemoës, M., Ploug, M., Boomsma, W., Kragelund, B.B., (2019). The PCNA interaction motifs revisited: thinking outside the PIP-box. *Cell. Mol. Life Sci.* **76**, 4923–4943.
38. Slade, D., (2018). Maneuvers on PCNA rings during DNA replication and repair. *Genes* **9**, 416.
39. Subramanian, J., Vijayakumar, S., Tomkinson, A.E., Arnheim, N., (2005). Genetic instability induced by overexpression of DNA ligase I in budding yeast. *Genetics* **171**, 427–441.
40. Lau, P.J., Flores-Rozas, H., Kolodner, R.D., (2002). Isolation and characterization of new proliferating cell nuclear antigen (POL30) mutator mutants that are defective in DNA mismatch repair. *Mol. Cell. Biol.* **22**, 6669–6680.

41. Haracska, L., Kondratick, C.M., Unk, I., Prakash, S., Prakash, L., (2001). Interaction with PCNA is essential for yeast DNA polymerase eta function. *Mol. Cell* **8**, 407–415.
42. Bruning, J.B., Shamoo, Y., (2004). Structural and thermodynamic analysis of human PCNA with peptides derived from DNA polymerase-delta p66 subunit and flap endonuclease-1. *Structure* **12**, 2209–2219.
43. Hishiki, A., Hashimoto, H., Hanafusa, T., Kamei, K., Ohashi, E., Shimizu, T., Ohmori, H., Sato, M., (2009). Structural basis for novel interactions between human translesion synthesis polymerases and proliferating cell nuclear antigen. *J. Biol. Chem.* **284**, 10552–10560.
44. Sebesta, M., Cooper, C.D.O., Ariza, A., Carnie, C.J., Ahel, D., (2017). Structural insights into the function of ZRANB3 in replication stress response. *Nature Commun.* **8**, 15847.
45. Duffy, C.M., Hilbert, B.J., Kelch, B.A., (2016). A disease-causing variant in PCNA disrupts a promiscuous protein binding site. *J. Mol. Biol.* **428**, 1023–1040.
46. Nair, A.G., Rabas, N., Lejon, S., Homiski, C., Osborne, M. J., Cyr, N., Sverzhinsky, A., Melendy, T., Pascal, J.M., Laue, E.D., Borden, K.L.B., Omichinski, J.G., Verreault, A., (2022). Unorthodox PCNA binding by chromatin assembly factor 1. *Int. J. Mol. Sci.* **23**, 11099.
47. Ben-Shahar, T.R., Castillo, A.G., Osborne, M.J., Borden, K.L.B., Kornblatt, J., Verreault, A., (2009). Two fundamentally distinct PCNA interaction peptides contribute to chromatin assembly factor 1 function. *Mol. Cell. Biol.* **29**, 6353–6365.